research articles Journal of proteome research

Differential Phosphoproteomics of Fibroblast Growth Factor Signaling: Identification of Src Family Kinase-Mediated Phosphorylation Events

Debbie L. Cunningham,[†,‡] Steve M. M. Sweet,[†,‡,§] Helen J. Cooper, and John K. Heath*[,‡]

School of Biosciences, College of Life and Environmental Sciences, University of Birmingham, Edgbaston, Birmingham, B15 2TT, United Kingdom

Received November 16, 2009

Activation of signal transduction by the receptor tyrosine kinase, fibroblast growth factor receptor (FGFR), results in a cascade of protein−protein interactions that rely on the occurrence of specific tyrosine phosphorylation events. One such protein recruited to the activated receptor complex is the nonreceptor tyrosine kinase, Src, which is involved in both initiation and termination of further signaling events. To gain a further understanding of the tyrosine phosphorylation events that occur during FGF signaling, with a specific focus on those that are dependent on Src family kinase (SFK) activity, we have applied SILAC combined with chemical inhibition of SFK activity to search for phosphorylation events that are dependent on SFK activity in FGF stimulated cells. In addition, we used a more targeted approach to carry out high coverage phosphopeptide mapping of one Src substrate protein, the multifunctional adaptor Dok1, and to identify SFK-dependent Dok1 binding partners. From these analyses we identify 80 SFK-dependent phosphorylation events on 40 proteins. We further identify 18 SFK-dependent Dok1 interactions and 9 SFK-dependent Dok1 phosphorylation sites, 6 of which had not previously been known to be SFK-dependent.

Keywords: phosphorylation • phosphopeptide • phosphoproteomics • phosphotyrosine • SILAC • quantitative mass spectrometry • FGFR • Src • Dok1

Introduction

The fibroblast growth factor (FGF) family of ligands and receptors execute a wide range of biological functions in development, tissue repair, angiogenesis and cellular homeostasis.[1−3] Dysregulation of the FGF signaling axis by a diversity of mechanisms is a frequent feature of a range of different tumor cell types[4,5] and, as a result, the FGF pathway is the target for the development of small molecule kinase inhibitors and other forms of therapeutic intervention.[2] However, to better inform the development of therapeutic interventions in the FGF pathway, and analyze their molecular actions, a complete understanding of the architecture of the downstream processes activated by FGF signaling is required. In this study we apply a differential phosphoproteomics approach to the identification of phosphorylation events mediated during activation of FGFR signaling.

Current understanding of the FGF signaling pathway holds that, following receptor dimerization by ligand engagement, activation of the intrinsic receptor tyrosine kinase leads to phosphorylation of key tyrosine residues on the receptor itself and the receptor-associated docking protein FRS2.[6,7] These phosphorylation events provide the basis for recruitment of effector proteins bearing sequence-specific phosphotyrosine recognition domains, which leads to further recruitment of downstream effectors and activation of intracellular signaling processes. The most prominent pathways associated with this mechanism are activation of the Ras/Raf/ERK pathway via recruitment of the adaptor protein Grb2 and the RasGEF SOS[8,9] activation of the PI3 kinase/PDK/Akt pathway via recruitment of the adaptor protein Gab1[10,11] and activation of phospholipase C via direct recruitment, via its SH2 domain, to the receptor.[12] Recent studies have provided further elaboration of this core pathway. A targeted mass spectrometric analysis of proteins that interact with activated FGFRs[13] identified a plethora of proteins associated with intracellular vesicular trafficking. One such partner, the small GTPase Rab5, has been shown to be crucial for sustaining propagation of the Ras/Raf/ERK, but not the PI3K/PDK/Akt signal. Additionally the non receptor tyrosine kinase c-Src has been shown to be rapidly recruited to the activated receptor complex, and Src kinase activity is required for both the initiation of FGF signaling and termination of the Ras/Raf/ERK pathway but not the PI3K/PDK/Akt pathway.[14] These findings point to the existence of further, as yet uncharacterized, mediators of FGFR signaling that are targets for Src kinase-mediated phosphorylation and functionally implicated in FGFR trafficking of activated FGFRs.

* To whom correspondence should be addressed. Prof. John K. Heath, School of Biosciences, College of Life and Environmental Sciences, University of Birmingham, Edgbaston, Birmingham B15 2TT, U.K. Telephone: +44 (0)121 414 7533. Fax: +44 (0)121 414 5925. Email: J.K.Heath@bham.ac.uk.
† These authors contributed equally to this work.
‡ Cancer Research UK Growth Factor Signalling Group.
§ Current address: Department of Chemistry, University of Illinois at Urbana−Champaign, Urbana, IL 61801.

10.1021/pr9010475

Published on Web 03/12/2010

During recent years, phosphoproteomic studies have successfully identified large numbers of phosphorylation sites.[15−17] This success is due in large part to efficient enrichment techniques for phosphopeptides and improvements in mass spectrometric instrumentation.[18] To obtain more biologically informative results from these types of studies, some form of quantitation can be applied.[19] In particular, stable isotope labeling with amino acids in cell culture (SILAC) is capable of quantifying even relatively subtle changes in protein levels.[20,21] Recently, software has been designed specifically to both improve SILAC data analysis and to cope with the large data sets generated from these experiments.[22]

In this study, we set out to identify further direct and indirect phosphorylation events on protein targets for Src family kinases (SFKs) downstream of FGFR using ultrahigh resolution mass spectrometry techniques.[23] Previous proteomic studies of the FGFR tyrosine kinase pathway have relied on overexpression of FGFR.[13,24,25] Rather than overexpress FGFR, we chose to combine FGF stimulation with pervanadate treatment to maximize the levels of tyrosine phosphorylated substrates. A similar approach using pervanadate treatment has been used in previous phosphoproteomics studies.[21,26−28] We applied SILAC combined with chemical inhibition of SFK activity to search for phosphorylation events that are dependent on SFK activity in FGF stimulated cells. SILAC has previously been used to study Src-substrates in cells overexpressing Src,[28] in Src-transformed cells,[29] and using chemical inhibition of SFK activity downstream of the PDGF receptor.[30] However, much of the data obtained identifies proteins as tyrosine phosphorylated without localizing the exact site of phosphorylation, and information regarding regulation on specific tyrosine phosphorylation sites of Src substrates is lacking.

Here, we identify 80 SFK-dependent phosphorylation events on 40 target proteins, including known Src substrates, downstream kinases and adaptor proteins. To illustrate further application of SILAC techniques to characterization of specific SFK-mediated phosphorylation events, we used a more targeted approach to carry out high coverage phosphopeptide mapping of one Src substrate protein, the multifunctional adaptor Dok1, and to identify SFK-dependent Dok1 binding partners.

Collectively, these results significantly expand the range of proteins implicated in the FGF signaling pathway and reveal potential new targets for therapeutic intervention in FGF and Src signaling.

Experimental Procedures

Cell Culture. Mouse NIH 3T3s cells were cultured at 37 °C, 5% CO_2 in DMEM containing 2 mM L-Glutamine (Lonza), supplemented with 0.1 mg/mL streptomycin, 0.2 U/mL penicillin (Sigma), and 10% v/v donor bovine serum (Labtech International). Human embryonic kidney epithelial 293T cells were cultured as above; however, donor bovine serum was substituted for 10% v/v fetal calf serum (Labtech International).

SILAC Labeling. For SILAC labeling, NIH 3T3 cells were cultured in amino acid deficient DMEM (Thermo) supplemented with either 0.1 mg/mL isotopically normal L-Lysine and L-Arginine (Sigma) or "heavy" $^{13}C_6$ L-Lysine and $^{13}C_6$ $^{15}N_4$ L-Arginine (Goss Scientific), 10% dialyzed FBS (Thermo), 2 mM L-Glutamine, 0.1 mg/mL streptomycin, and 0.2 U/ml penicillin. 293T cells were cultured as above, with the addition of 0.5 mg/mL proline (Sigma) in the media.[31] Cells were grown for at least five doubling times prior to use in order for the cells to fully incorporate the labeled amino acids.

Cloning and Transfection. The human open reading frame for Dok1 was supplied in a Gateway (Invitrogen) pDONR vector from Open Biosystems. The insert encoding Dok1 was cloned into the Gateway compatible mammalian expression vector, Myc-PRK5 (gift from Laura Machesky) using Gateway cloning. Cells were transfected using Genejuice (Novagen) according to manufacturers' instructions and allowed to overexpress transfected protein for 48 h.

Cell Treatment and Cell Lysis. Following overnight serum starvation in media containing 0.1% serum, cells were either pretreated with 25 μM SU6656 for 1 h, followed by addition of 2 mM sodium pervanadate for 20 min, and then 20 ng/mL FGF2 for 30 min, or treated as above in the absence of SU6656. Prior to lysis, cells were washed twice in cold phosphate-buffered saline (PBS) and then lysed at 4 °C in 1 mL lysis buffer (50 mM Tris-HCl pH 7.4, 150 mM NaCl, 1 mM EDTA, 1% Triton X-100 (w/v), 1 mM Na_3VO_4, 50 mM NaF, 25 mM β-glycerophosphate and 1 tablet of protease inhibitor mixture (Roche Molecular Diagnostics) per 10 mL of buffer) per 175-cm^2 flask of cells. After incubation on ice for 30 min, the lysates were centrifuged at 15 000$\times$ g at 4 °C for 20 min. Total protein concentrations of the cleared lysates were then determined using the Coomassie (Bradford) Protein Assay Kit (Pierce Biotechnology Inc.), according to the manufacturers' instructions.

Western Blotting. Whole cell lysates were run on 4−12% Bis-Tris gels (Invitrogen). Protein was transferred to FL polyvinylidene difluoride membrane (Millipore Corp.) at 100 V for 1 h 15 min. To block the membranes they were washed in methanol and allowed to dry. Primary antibodies were incubated with the membrane overnight at 4 °C in Odyssey Blocking Buffer (Licor Biosciences) containing 0.1% Tween-20. The blot was washed three times for 15min in PBS/0.1% Tween-20 (PBS-T) and probed with the IRDye conjugated secondary antibody (Licor Biosciences) diluted in Odyssey Blocking Buffer/0.1% Tween-20/0.01% SDS for 1 h at room temperature, in the dark. The membrane was washed three times in PBS-T, followed by a final wash in PBS (no Tween 20). Membranes were visualized using fluorescence detection on the Odyssey Infared Imaging System (Licor Biosciences). Primary antibodies used in this study were obtained from Santa Cruz (FRS2, ERK, ERK pY204) and Cell Signaling Technology (FGFR1 pY653/pY654, FRS2 pY196, Src, Src pY416, AKT, and AKT pT308).

Immunoprecipitation. For the phosphotyrosine immunoprecipitation (IP), agarose-conjugated antiphosphotyrosine (clone 4G10) antibody (Upstate) was used. Whole cell lysates (WCL) were initially precleared with protein A agarose beads for 30 min at 4 °C (25 mg/100 μL beads) before mixing with antibody-conjugated beads (25 mg WCL/100 μL beads). Following overnight incubation at 4 °C, beads were washed six times in a 100-fold excess of ice-cold PBS. To address reproducibility, four replicates of the SILAC phosphotyrosine IPs were carried out. For Myc-Dok1 IPs, Myc-Dok1 antibody 9E10 (Roche) was conjugated to Protein G Dynabeads, as per manufacturers' instructions (Invitrogen; 10 μg Ab/25 μL Dynabeads), prior to addition of cell lysate. WCLs (10 mg) from the heavy and light cell populations were immunoprecipitated separately. WCLs were mixed at 4 °C with conjugated beads (10 mg/170 μL conjugated beads) for 1 h and beads were washed twice in a 20-fold excess of lysis buffer. Beads from both "heavy" and "light" IPs were then mixed and washed a further three times, again in a 20-fold excess of lysis buffer. Following addition of reduced sample buffer, protein samples were run on 4−12% Bis-Tris gels (Invitrogen) and Coomassie

stained. Two replicates of each Myc-Dok1 IP were carried out and samples from each IP were analyzed in duplicate.

Trypsin Digestion and Phosphopeptide Enrichment of Samples. Following the phosphotyrosine IPs, the agarose-conjugated beads were resuspended in 8 M urea, 50 mM ammonium bicarbonate. The beads were then heated at 95 °C for 5 min and eluted proteins were removed in the supernatant after centrifugation. The protein mixtures were diluted to 1 M urea, reduced (4 mM DTT) and alkylated (8 mM iodoacetamide) in 50 mM ammonium bicarbonate prior to overnight trypsin digestion (1:100 enzyme:protein; Trypsin Gold; Promega, Madison, WI).

Following the Myc-Dok1 IPs, excised bands from Coomassie-stained gels were destained, reduced (10 mM DTT) and alkylated (55 mM iodoacetamide) in 25 mM ammonium bicarbonate prior to overnight in-gel trypsin digestion (12.5 ng/μL; Trypsin Gold; Promega, Madison, WI).

Digested samples were acidified by addition of trifluoroacetic acid (0.5% final volume). Peptides from the anti-pY IPs were desalted (Peptide concentration and desalting Macrotrap; Michrom Bioresources, Pleasanton, CA) and dried by vacuum centrifugation. Phosphopeptides were enriched using TiO_2 as described.[23] The resulting peptide mixtures were analyzed by liquid chromatography tandem mass spectrometry (LC−MS/MS).

Mass Spectrometry. Online liquid chromatography was performed by use of a Micro AS autosampler and Surveyor MS pump (Thermo Electron, Bremen, Germany). Peptides were loaded onto a 75 μm (internal diameter) Integrafrit (New Objective, Woburn, MA) C8 resolving column (length 10 cm) and separated over a 40 min gradient from 0% to 40% acetonitrile (Baker, Holland). Peptides eluted directly (~300 nL/min) via a Triversa nanospray source (Advion Biosciences, Ithaca, NY) into a 7 T LTQ FT mass spectrometer (Thermo Fisher Scientific). The mass spectrometer alternated between a full FT-MS scan (m/z 395−1600), subsequent CID MS/MS scans of the five most abundant ions, and, if a neutral loss of 98 Da from the precursor ion was observed in the CID mass spectrum, an MS^3 scan of the neutral loss ion. Survey scans were acquired in the ICR cell with a resolution of 100 000 at m/z 400. Precursor ions were isolated and subjected to CID in the linear ion trap. Isolation width was 3 Th. Only multiply charged precursor ions were selected for MS/MS. CID was performed with helium gas at a normalized collision energy of 35%. Precursor ions were activated for 30 ms. Data acquisition was controlled by Xcalibur 2.0 software.

Identification and Quantification of Peptide and Proteins. Mass spectra were processed using the MaxQuant software (version 1.0.12.31).[22,32] Data were searched, using MASCOT version 2.2 (Matrix Science), against a concatenated database consisting of the mouse or human IPI database supplemented with common contaminants (including keratins, trypsin, BSA) and the reversed-sequence version of the same database. The mouse database contained 111 130 protein entries (55 565 of which were reversed-sequence versions). The human database contained 148 380 protein entries (74 190 of which were reversed-sequence versions). The search parameters were: minimum peptide length 6, peptide tolerance 30 ppm, mass tolerance 0.5 Da, cleavage enzyme trypsin/P, and a total of 2 missed cleavages were allowed. Carbamidomethyl (C) was set as a fixed modification and oxidation (M) and acetylation (Protein N-term) were set as variable modifications. When searching for phosphopeptides, Phospho (ST) and Phospho (Y) were also set as variable modifications. The appropriate SILAC labels were selected and the maximum labeled amino acids was set to 3.

For identification of phosphorylation sites, all experiments (phosphotyrosine IP and Myc-Dok1 IP) were filtered to have a peptide false-discovery rate (FDR) below 1%. The Myc-Dok1 IP experiments were further required to have a protein FDR below 1%. Within the MaxQuant output, phosphorylation sites were considered to be localized correctly if the localization score (PTM score) was at least 0.80 (80%). Further parameters and settings are detailed in the Supplementary Methods.

Phosphorylation Site Localization using SLoMo. DTA files were created from the raw data using Bioworks 3.3.1 (Thermo Fisher Scientific Inc.). The DTA files were searched using Mascot with the search parameters as described above. Mascot search results were exported as a pepxml file and this file was analyzed using the SloMo software.[35]

Results and Discussion

Identification of Src Family Kinase-Mediated Phosphorylation Events, in the Presence of FGF2. Activation of fibroblast growth factor receptors (FGFRs) by FGF2 initiates a cascade of reversible phosphorylation events on both the receptor and on downstream effector proteins.[6] Although the core signaling events during FGFR signaling are well established, relatively little has been published on the global analysis of changes in protein levels and phosphorylation events.[13,24,25] Our aim was to generate a data set of tyrosine phosphorylated proteins that could be mapped to the FGF signaling pathway.

We have chosen to focus specifically on a network of proteins that may be involved in FGFR trafficking and endocytosis: the Src-mediated network. Src family kinases (SFKs) have long been implicated in signaling by a variety of receptor tyrosine kinases (RTKs), including FGFR, epidermal growth factor receptor (EGFR), insulin-like growth factor-1 receptor (IGF-1R), and hepatocyte growth factor (HGFR).[34] In FGFR signaling, upon activation of receptor by FGF2, Src is recruited via the adaptor protein, FRS2 and also becomes activated.[14,35] Active Src then plays a role in regulation of the activation and transport of FGFR from and to the plasma membrane via the Src-regulated endosomal-actin pathway.[14,36] Considering the role of Src in trafficking of FGFRs, we decided to further characterize SFK-mediated phosphorylation events that may be downstream of FGFR, using a SILAC quantitative phosphoproteomics approach coupled with chemical inhibition of SFK activity.

Prior to FGF2 stimulation, cells were treated with sodium pervanadate to inhibit tyrosine phosphatase activity, thereby increasing the levels of transiently phosphorylated phosphotyrosine proteins.[27] As phosphorylation events are the result of a balance between kinase and phosphatase activities, inhibition of phosphatase activity will allow a history of kinase-mediated phosphorylation events to remain during the course of the experiment. Activation of FGFR, as measured by phosphorylation on residues 653 and 654, is rapid in response to FGF2 and peaks between 3 and 10 min (Figure 1). Phosphorylation of well-characterized downstream target proteins of FGFR, such as FRS2, Src, AKT and ERK peaks between 10 and 30 min. We chose to stimulate NIH 3T3 cells with FGF2 for 30 min, in the presence or absence of the selective Src family kinase inhibitor, SU6656,[37] in order to investigate phosphorylation events downstream of FGFR-dependent phosphorylation of SFKs. This was followed by quantitative analysis of the SFK-dependent phosphorylation events. Without overexpressing

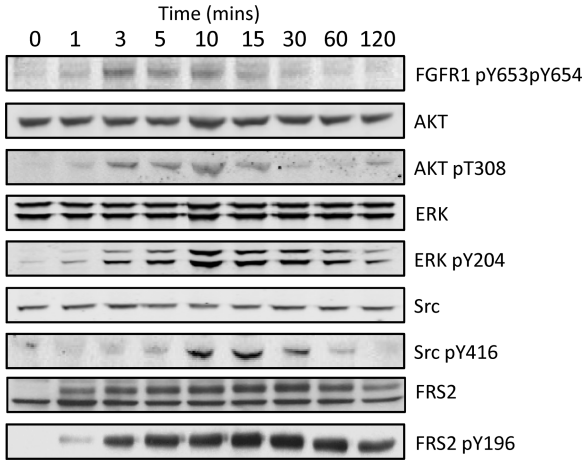

Figure 1. Profiles of phosphorylation events in the presence of FGF2. NIH 3T3s were stimulated with 20 ng/mL FGF2 for varying lengths of time. Western blot analysis was carried out on whole cell lysates using antibodies against indicated proteins and phospho-proteins.

FGFR, as has been done previously to study the phosphoproteome of FGF signaling,[24,25] and in the absence of pervanadate treatment, levels of phosphopeptides remained too low for mass spectrometric detection (data not shown).

We performed four independent experiments, three utilizing both heavy arginine and lysine SILAC labels and one utilizing only heavy lysine. From these experiments we identified 711 (redundant) peptides, including 430 (redundant) phosphotyrosine peptides (Supplementary Table S1, Supporting Information). Representative mass spectra for two of the identified phosphopeptides are shown in Figure 2 (see Supporting Information for additional spectra). Given the complexity of the starting sample (mouse whole cell lysate) and the variability introduced during the phosphotyrosine IP and phosphopeptide enrichment steps, we expected considerable variation between experiments. The overlap between the four experiments is shown in Figure S1 (Supporting Information): 50% of the phosphotyrosine peptides were identified in 2 or more experiments, while 30% were identified in 3 or more experiments. A total of 131 unique tyrosine phosphorylation sites were identified from 63 distinct proteins. Of the total 131 phosphotyrosine sites, 6 (5%) are novel, unpublished sites according to the PhosphoSitePlus database at www.phosphosite.org.[38]

Of the peptides identified, a total of 506 were assigned a SILAC ratio in MaxQuant, the remainder were not, due to peptide levels being undetectable in one of the cell populations or due to the peptide not containing a lysine (singly labeled experiment). The three experiments utilizing both arginine and lysine SILAC labels gave a total of 433 phosphopeptide identifications, of which 303 were tyrosine phosphorylated and were assigned a SILAC ratio (Supplementary Table S2, Supporting Information). The overlap between these three experiments for the 303 phosphotyrosine peptides (139 nonredundant phosphotyrosine peptides) is shown in Figure S2 (Supporting Information): again, 50% of the phosphotyrosine peptides were identified in two or more experiments and 25% were identified in all three experiments.

A total of 80 tyrosine phosphorylation sites show a significant ($p < 0.05$) increase or decrease in abundance in the phosphotyrosine immunoprecipitates due to the presence of the SFK inhibitor (Table 1). Several of the SFK-dependent tyrosine phosphorylation sites identified are on proteins known to be regulated by Src, including BAIP2, ZO1, paxillin, caveolin, Dok1, EGFR, Eps8, STAM2, cortactin, FAK1, PDGFRα, p130Cas, p120 catenin, tensin, PLCγ, and SHIP2.[28,39−41] This validates the strength of our approach for identifying Src-targets. For many of these proteins, the specific site(s) of tyrosine phosphorylation have not been previously identified as SFK phosphorylation sites according to the Human Protein Reference Database.[42] Furthermore, our data agrees with previous phosphoproteomic studies that have examined the phosphotyrosine peptide profile in 3T3 mouse fibroblasts expressing a constitutively active Src mutant, SrcY529F[26,29] in that we identify several Src-dependent phosphotyrosine sites that were also frequently identified in these Src-transformed cells. These include: p120 catenin pY96, pY221, pY228, pY257, pY280; p130cas pY132; Dok1 pY295; cortactin pY215, and ZO1 pY1164, pY1177.

Abi1, CDV3, afadin, and LPP have been identified as possible Src substrates in a previous phosphoproteomic study using SILAC to compare tyrosine phosphorylated proteins in SW60-Src with those in SW60 cells.[28] Our data provides further evidence that these proteins are Src substrates and also maps the specific phosphorylation sites on these proteins that are regulated by Src.

In addition, a large percentage (>30%) of the Src-dependent phosphotyrosine sites were found in proteins not previously reported to be regulated by Src. These include the proteins ABLM1, CASL, Cadherin-11, Drebrin-like protein, Emerin, PARD3, PEAR1, RMB3, and TERA.

We have not used overexpression of FGFR in these studies; therefore, we do not expect complete overlap with previous phospho-proteomic studies of FGF signaling that have relied on overexpressed FGFR.[24,25] Ten FGFR1-associated tyrosine phosphorylated proteins were identified in these overexpression studies of which four were identified here as SFK-substrates (cortactin, p130Cas, PLCγ and paxillin). Tyrosine phosphorylation of these proteins, therefore, appears to be both downstream of FGFR and SFK activation. An additional 20 proteins were shown to be enriched in a phosphotyrosine IP as a consequence of FGF-stimulation, however, tyrosine phosphorylation sites were not identified.[24] Of these additional proteins, we identify both FAK1 and SHIP2 as SFK-substrates, and also RSK2.

Src Family Kinase-Dependent Dok1 Phosphorylation Sites. Although the global SFK-dependent phosphorylation data set provides evidence for SFK-mediated tyrosine phosphorylation on a large number of proteins, it provides limited mapping of phosphorylation sites on individual proteins. This is not unexpected, given the limited dynamic range of proteomic experiments and can be addressed through targeted analysis of particular proteins, enabling identification of lower stoichiometry sites of phosphorylation. We apply this further step to localize additional sites of phosphorylation on the protein Dok1. We note, however, that this step in our approach can be used to further characterize any of the proteins showing SFK-dependency that we have identified in our global analysis.

We chose to study Dok1 based on its reported interaction and regulation by Src[43−46] and also its role in tyrosine kinase receptor mediated signaling.[45,47,48] Dok1 is an adaptor protein involved in protein complex formation during cell signaling and is a substrate for many protein tyrosine kinases. Dok1 is known to be phosphorylated by activated Src[43,45,46] and also by activated EGF receptor[45] and insulin receptor.[47,48] Upon tyrosine phosphorylation, Dok1 recruits a variety of SH2-contain-

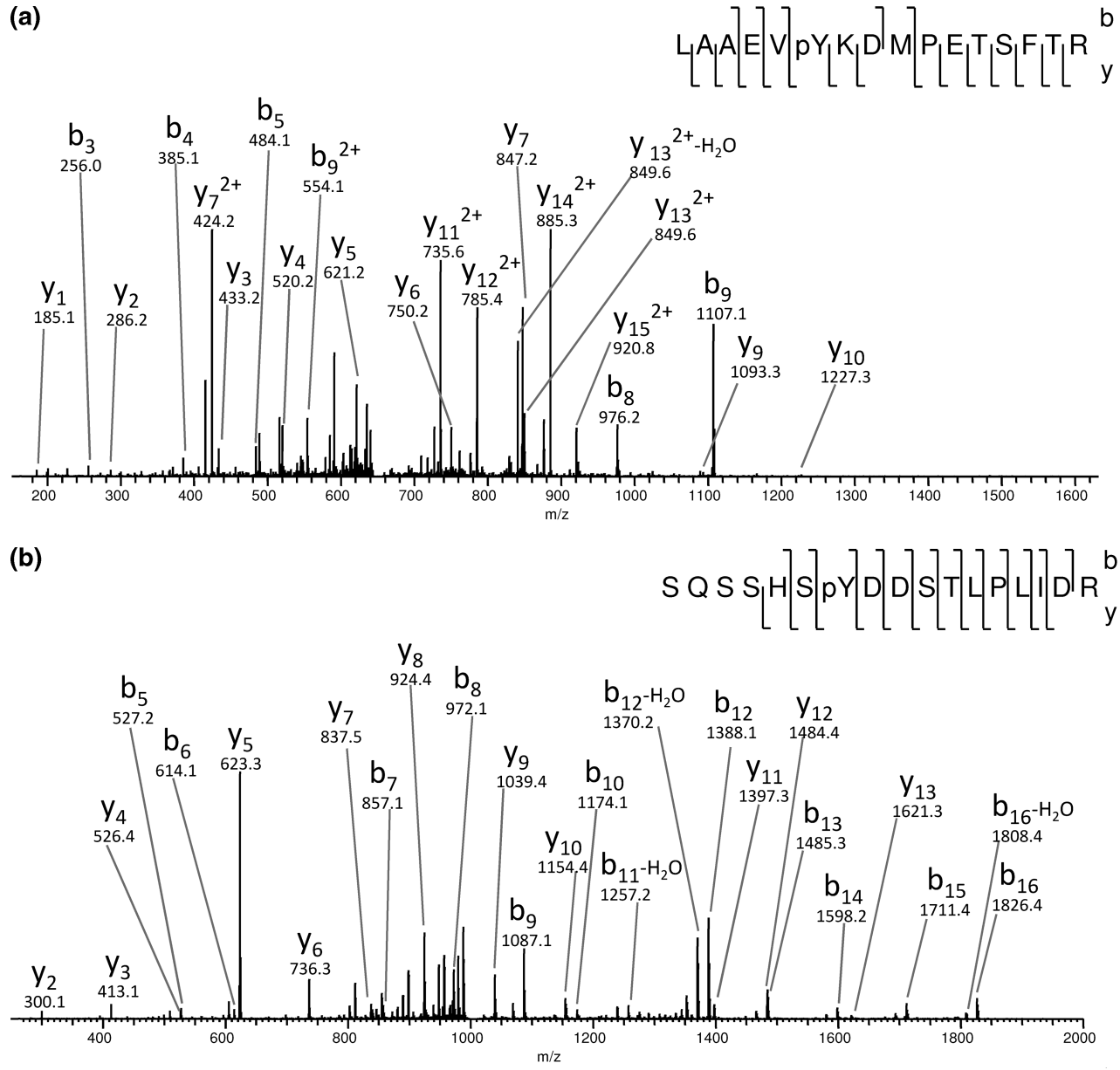

Figure 2. Representative mass spectra for identification and site localization of tyrosine phosphorylation. (a) Afadin is phosphorylated at pY203. (b) Catenin delta-1 is phosphorylated at pY865. Peptides are labeled with 13C(6),15N(4) Arg and 13C(6) Lys. pY indicates phosphotyrosine.

ing proteins and is therefore an attractive candidate for mediation of FGF signaling.

To map phosphorylation sites of Dok1 and determine which of these phosphorylation events are SFK-dependent, we carried out a SILAC experiment in which Myc-Dok1 was overexpressed and immunoprecipitated in 293T cells. Heavy and light populations were stimulated with sodium pervanadate and FGF2 ± SU6656, as described above. Phosphopeptide enrichment was carried out on the immunoprecipitated Dok1.

The potential for distinct phosphorylation sites with distinct patterns of regulation on the same tryptic peptide is an important factor to take into account when analyzing data such as these.[49] Initial examination of the MaxQuant output revealed several identical peptides with a number of possible phosphorylation sites. In one particular case, the peptide, LPSPPGPQELLDSPPALYAEPLDSLR was separately identified as being phosphorylated on the first serine, the second serine, or the tyrosine residue. The SILAC ratios were highly variable between peptides where the phospho-group had been allocated the same localization, and after averaging ratios for each modification the data suggested that the SILAC ratios were all unchanged in the presence of SU6656. These data prompted us to use the SLoMo software[33] to reanalyze the site-localization on these enriched Dok1 phosphopeptides. Analysis of the SLoMo output reveals that the three phosphopeptides are indeed present and are partially coeluting. Further manual inspection of the spectra reveals that only the phosphotyrosine version is differentially regulated in the presence of SU6656 (Figure 3).

A total of 12 distinct sites of phosphorylation (4 serines, and 8 tyrosines) on Dok1 were identified. According to the PhosphositePlus database,[38] all but one has been published

Table 1. Phosphotyrosine Peptides Significantly Changed Due to the Presence of SU6656[a]

protein	phosphopeptide	phosphosite(s)	SILAC ratio	% variability
ABI1 Abelson interactor 1	NTPpYKTLEPVKPPTVPNDpYMTSPAR	pY197, pY212	0.083	56.942
	TLEPVKPPTVPNDpYMTSPAR	pY212	0.561	79.405
ABLM1 Actin-binding LIM protein 1	STSQGSINSPVpYSR	pY505	0.195	
AFAD Afadin	LAAEVpYKDMPETSFTR	pY203	0.259	85.353
	EpYFTFPASK	pY1230	0.482	41.237
	SQEELREEKVpYQLER	pY1285	0.202	43.666
AHNAK Ahnak protein	VKGEpYDVTMPK	pY963	0.316	
BAIP2 Insulin receptor substrate p53	LSDSpYSNTLPVRK	pY338	0.164	
BCAR1 p130cas	TQQGLpYQAPGPNPQFQSPPAK	pY132	0.221	
	GLLSSSHHSVpYDVPPSVSK	pY310	0.577	22.478
	RPGPGTLpYDVPR	pY391	0.326	23.664
CASL CRK-associated substrate-related protein	LpYQVPNSQAASR	pY91	0.352	38.486
CAV1 Caveolin-1	YVDSEGHLpYTVPIR	pY14	0.378	3.108
CDH11 Cadherin-11	KDIKPEpYQYMPR	pY700	0.265	13.550
CDV3 Protein CDV3	KTPQGPPEIpYSDTQFPSLQSTAK	pY213	0.143	33.332
	LQLDNQpYAVLENQK	pY267	0.162	
CTND1 Catenin delta-1	LNGPQDHNHLLpYSTIPR	pY96	0.530	32.209
	TVQPVPMGPDGLPVDASAVSNNpYIQTLGR	pY174	0.382	17.762
	NFHYPPDGYGRHYEDGpYPGGSDNpYGSLSR	pY221, pY228	0.173	23.705
	HYEDGYPGGSDNpYGSLSR	pY228	3.003	21.770
	YRPSMEGpYR	pY248	0.155	44.702
	QDVpYGPQPQVR	pY257	0.254	30.310
	FHPEPpYGLEDDQR	pY280	0.289	60.708
	SQSSHSpYDDSTLPLIDR	pY865	0.116	45.682
	SLDNNpYSTLNERGDHNR	pY904	0.429	35.851
DBNL Actin-binding protein 1	ESTSFQDVGPQAPVGSVpYQK	pY162	0.092	18.622
	QLTQPETSpYGREPTAPVSR	pY305	0.044	53.280
DOK1 Docking protein 1	TVPPPVPQDPLGSPPALpYAEPLDSLR	pY295	0.579	19.218
E41L3 Band 4.1-like protein 3	SLDGEVGTGQpYATTK	pY453	0.353	
EGFR Epidermal growth factor receptor	LLGAEEKEpYHAEGGKVPIK	pY871	0.203	40.247
	RPAGSVQNPVpYHNQPLHPAPGR	pY1110	0.385	39.984
	GPTAENAEpYLR	pY1197	0.555	44.154
EMD Emerin	TpYGEPESVGMSK	pY106	0.074	25.481
	LIYGQDSApYQSIAHYRPISNVSR	pY161	0.089	33.376
	LIYGQDSAYQSIAHpYRPISNVSR	pY167	0.054	
EPS8 Epidermal growth factor receptor kinase	STPNHQVDRNpYDAVK	pY524	0.504	
FAK1 Focal adhesion kinase 1	AAApYLDPNLNHTPSSSTK	pY4	0.174	21.969
	YMEDSTpYpYKASK	pY614, pY615	0.343	15.339
IFITM3 Interferon-induced transmembrane protein 3	MNHTSQAFITAASGGQPPNpYER	pY20	0.576	18.836
	IKEEpYEVAEMGAPHGSASVR	pY27	0.433	26.578
KIRR1 Kin of IRRE-like protein 1	AVLpYADYRAPGPTR	pY654	2.348	
	AVLYADpYRAPGPTR	pY657	0.350	
	AVLpYADpYRAPGPTR	pY654, pY657	0.432	19.452
	TPpYEApYDPIGK	pY753, pY756	0.467	
	TPYEApYDPIGK	pY756	1.771	20.387
	FSYTSQHSDpYGQRFQQR	pY777	0.484	
LPP Lipoma-preferred partner homologue	SAQPSPHpYMAGPSSGQIpYGPGPR	pY235, pY245	0.032	173.794
	SAQPSPHYMAGPSSGQIpYGPGPR	pY245	0.063	111.089
	YpYEPYYAAGPSYGGR	pY297	0.266	
	YYEPYpYAAGPSYGGR	pY302	0.269	10.928
	SEGDTApYGQQVQPNTWK	pY318	0.137	96.380
	EAApYAPPASGNQNHPGMYPVSGPK	pY333	0.071	65.503
PARD3 Partitioning-defective 3 homologue	ESVSTSSDQPSpYSLER	pY969	0.118	
	ERDpYAEIQDFHR	pY1076	0.514	16.397
PAXI Paxillin	YAHQQPPSPLPVpYSSSAK	pY88	0.395	31.523
	AGEEEHVpYSFPNK	pY118	0.501	24.616
PCDHGC3 Protocadherin gamma C3	APVSSLpYR	pY735	0.528	
PEAR1 Platelet endothelial aggregation receptor 1	ESGpYVEMKGPPSVSPPR	pY41	0.138	
PGFRA Platelet-derived growth factor receptor alpha	QADTTQpYVPMLER	pY742	0.443	32.533
	SLpYDRPASYK	pY762	0.410	32.001
	LSADSGpYIIPLPDIDPVPEEEDLGKR	pY1018	0.162	38.489
PKP4 Plakophilin-4	LQHQQLpYpYQDDSTRK	pY1114, pY1115	0.387	5.041
PLCG1 PLCγ	pYQQPFEDFR	pY1253	0.518	5.699
Q3UGC2 Cortactin, isoform CRA_e	HESQQDpYAKGFGGK	pY302	0.291	17.822
RBM3 RNA-binding motif protein 3	YDSRPGGYGpYGYGR	pY124	0.204	
	YSGGNYRDNpYDN	pY151	0.318	44.561
SCAM3 Scamp3	NpYGSYSTQASAAAATAELLK	pY85	0.333	30.094
SHIP2 Phosphatidylinositol-3,4,5-trisphosphate 5-phosphatase 2	TLSEVDpYAPGPGR	pY1136	0.560	31.372
STAM2 Signal transducing adapter molecule 2	LVNEAPVpYSVYSK	pY371	0.113	27.025
SRC8 Cortactin	HASQKDpYSSGFGGK	pY154	0.201	
	NASTFEEVVQVPSApYQK	pY334	0.085	32.432
TBCB Tubulin folding cofactor B	LGEpYEDVSKVEK	pY98	0.172	
TENC1 Tensin-2	GPLDGSPpYAQVQR	pY483	0.245	38.913
	LALPTAALpYGLR	pY705	0.204	
TENS1 Tensin-1	HAApYGGYSTPEDR	pY1477	0.293	
TERA Transitional endoplasmic reticulum ATPase	GFGSFRFPSGNQGGAGPSQGSGGGT GGSVYTEDNDDDLpYG	pY805	0.111	
ZDHC8 Probable palmitoyltransferase ZDHHC8	KVSGVGGTTpYEISV	pY711	0.432	
ZO1 Tight junction protein ZO-1	YRPEAQPpYSSTGPK	pY1177	0.038	62.278
	SpYEQVPPPGFTSK	pY1198	0.208	58.171
	HEEQPAPApYEVHNR	pY1164	0.112	50.945

[a] Variability (%) was calculated using the standard deviation of the natural logarithms of the SILAC ratios, multiplied by 100.

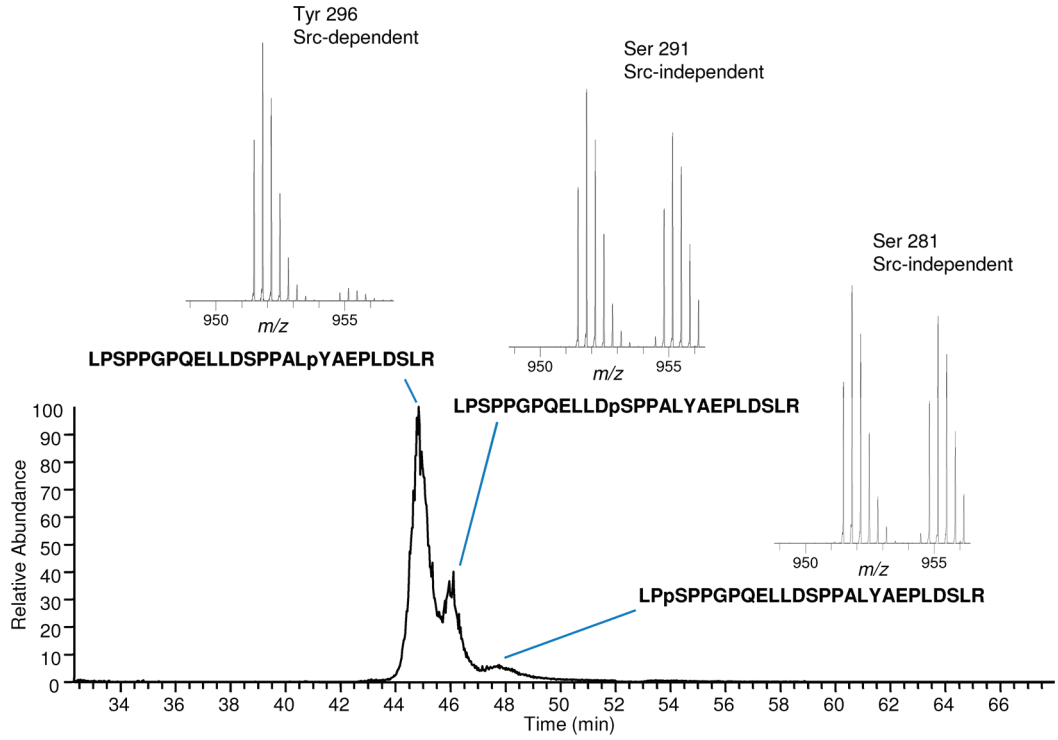

Figure 3. Partial co-elution of isobaric phosphopeptides. The Dok1 peptide LPSPPGPQELLDSPPALYAEPLDSLR is present in three different singly phosphorylated forms, with phosphorylation occurring at Ser281, Ser291, and Tyr296. The selected-ion chromatogram for the $[M + 3H]^{3+}$ light precursor is shown. Comparison of the heavy/light ratios for the three versions indicates that only Tyr296 is Src-dependent.

Table 2. Phosphopeptide Mapping of Dok1[a]

phosphosite(s)	modified peptide(s)	localization score (SLoMo)	ratio H/L count	ratio H/L	% variability
	Peptides with reduced SILAC ratios in the presence of SU6656				
Ser48	LEFFDHKGSpSSGGGR	25.6	2	0.377	3.308
Tyr296	LPSPPGPQELLDSPPALpYAEPLDSLR	75	3	0.136	108.796
Tyr337	KKPLpYWDLYEHAQQQLLK	62.1	2	0.033	38.622
Tyr341	KKPLYWDLpYEHAQQQLLKKPLYWDLpYEHAQQQLLK	100.4	10	0.018	76.261
Tyr362	EDPIpYDEPEGLAPVPPQGLYDLPRLTDPKEDPIpYDEPEGLAPVPPQGLYDLPR	142.5	9	0.198	16.081
Tyr377	EDPIYDEPEGLAPVPPQGLpYDLPRLTDPKEDPIYDEPEGLAPVPPQGLpYDLPR	185.5	5	0.099	142.837
Tyr398	VKEEGpYELPYNPATDDYAVPPPR	30.6	1	0.084	
Tyr409	EEGYELPYNPATDDpYAVPPPRVKEEGYELPYNPATDDpYAVPPPR	79.6	20	0.142	43.88
Tyr449	SHNSALpYSQVQK	72.1	21	0.167	118.322
Tyr337;Tyr341	KPLpYWDLpYEHAQQQLLK	One possibility	1	0.071	
Tyr362;Tyr377	LTDPKEDPIpYDEPEGLAPVPPQGLpYDLPR	18.6	4	0.030	60.981
Tyr398;Tyr409	VKEEGpYELPYNPATDDpYAVPPPR	34.1	3	0.024	23.142
	Peptides with unchanged SILAC ratios in the presence of SU6656				
Ser269	ADpSHEGEVAEGKAGQGHDVLRADpSHEGEVAEGK	One possibility	11	0.880	15.969
Ser281	LPpSPPGPQELLDSPPALYAEPLDSLR	39.7	5	0.772	30.703
Ser291	LPSPPGPQELLDpSPPALYAEPLDSLR	84.2	8	0.899	33.448

[a] SLoMo score $= -10 \times (\log(p))$. A score of 19 corresponds to a localization confidence with $p = 0.0126$.[33]

previously, the exception being Ser48. Out of the 12 identified phosphosites, 9 (Ser48, Tyr 296, Tyr337, Tyr341, Tyr362, Tyr377, Tyr398, Tyr409, Tyr449) had a significantly reduced SILAC ratio ($p < 0.05$; Table 2), indicating that these particular phosphorylation sites within Dok1 are regulated via Src family kinases.

Although many sites of phosphorylation have been previously identified on Dok1, only three tyrosine residues (Y296, Y362, and Y449) have been reported to be direct sites of Src-mediated phosphorylation, with residue 362 described as a binding site for Src.[46,50] We have identified these 3 tyrosine phosphorylation sites, together with a further 5 tyrosine residues whose phosphorylation is decreased in the presence of SU6656. In addition, the novel phosphoserine 48 residue that we have identified also shows SFK-dependency. Both Src-dependent phosphorylation sites of Dok1, and sites not previously identified as Src-dependent phosphorylation sites, have been implicated in recruitment of proteins. Phosphorylation

Table 3. Proteins with Increased SILAC Ratios Due to Enrichment in Myc-Dok1 Transfected Cells

protein IDs	protein names	unique peptides (seq/mod/labels)	sequence coverage (%)	ratio H/L	ratio H/L significance
IPI00306531	NCK2	6	9.5	2.626	4.27×10^2
IPI00449049	Poly [ADP-ribose] polymerase 1 (PARP1)	2	2.4	2.750	3.57×10^2
IPI00887678	Peptidyl-prolyl cis−trans isomerase A	6	27.4	2.762	3.51×10^2
IPI00007188	ADP/ATP translocase 2	11	25.8	3.070	2.27×10^2
IPI00293655	ATP-dependent RNA helicase DDX1	5	6.4	3.363	1.52×10^2
IPI00396435	Putative pre-mRNA-splicing factor ATP-dependent RNA helicase DHX15	2	1.5	3.391	1.47×10^2
IPI00296337	DNA-dependent protein kinase catalytic subunit	4	1.2	3.572	1.15×10^2
IPI00410693	Plasminogen activator inhibitor 1 RNA-binding protein	3	6.6	3.609	1.10×10^2
IPI00215790	60S ribosomal protein L38	4	47.1	3.842	8.11×10^3
IPI00386604	Putative uncharacterized protein	6	15	4.603	3.18×10^3
IPI00026781	Fatty acid synthase	7	3.3	5.025	1.95×10^3
IPI00018350	DNA replication licensing factor MCM5	6	10.6	5.671	9.55×10^4
IPI00376798	60S ribosomal protein L11	9	40.4	6.067	6.29×10^4
IPI00024067	Clathrin heavy chain 1	3	2.5	6.126	5.92×10^4
IPI00396485	Elongation factor 1-alpha 1	12	16	6.882	2.78×10^4
IPI00016610	Poly(rC)-binding protein 1	2	6.7	8.265	7.81×10^5
IPI00013214	DNA replication licensing factor MCM3	9	10.7	12.162	3.81×10^5
IPI00156005	RNA-binding protein Nova-2	1	2.2	19.196	5.92×10^8
IPI00013212	Tyrosine-protein kinase CSK	14	29.6	19.795	4.37×10^8
IPI00186290	Elongation factor 2	11	11.9	28.888	8.16×10^{10}
IPI00000874	Peroxiredoxin-1	8	43.2	30.256	4.86×10^{10}
IPI00216746	Heterogeneous nuclear ribonucleoprotein K	4	13.6	30.681	4.15×10^{10}
IPI00027350	Peroxiredoxin-2	4	27.8	31.323	3.28×10^{10}
IPI00011200	D-3-phosphoglycerate dehydrogenase	13	25.5	77.030	3.25×10^{15}
IPI00015287	Docking protein 1 (Dok1)	53	80.5	82.827	1.15×10^{15}

of residue 362 is involved in Nck recruitment,[48] and phosphorylation of Tyr296, Tyr315, Tyr362, Tyr398, and Tyr409, has been implicated in binding to Ras-GAP.[48,51,52]

Src Family Kinase-Dependent Dok1 Binding Partners. Using this targeted, quantitative SILAC method, not only have we identified SFK-dependent Dok1 phosphorylation sites, but, using the same IP sample we can also identify the SFK-dependency of Dok1 interactions with binding partners. In order to identify specific binding partners of Dok1 and to determine which proteins are present as a consequence of nonspecific interactions, we carried out a parallel SILAC experiment comparing untransfected cells with cells in which Myc-Dok1 was overexpressed. All cells were treated with sodium pervanadate and FGF2 as described above.

A total of 329 proteins were identified from the IP in which Myc-Dok1 transfected cells were compared to untransfected cells (Supplementary Table S3, Supporting Information). The false-discovery rate was controlled at below 1%. MaxQuant calculated SILAC ratios for 185 of these proteins. Proteins with SILAC ratios significantly different from the median, as calculated using MaxQuant ($p < 0.05$), were considered as enriched proteins in either cell population. Those proteins present equally in the transfected and untransfected samples or enriched in the untransfected cell population were considered as contaminants in further IP experiments. Table 3 shows the 25 proteins that were enriched in the 293T cells transfected with Dok1. Csk and NCK2, proteins known to interact with Dok1,[53,54] showed a significantly increased abundance in the 293T-Dok1 cells, as measured by their SILAC ratio. In addition, Grb2, RasGAP, and PLCγ1, all known Dok1 binding partners,[44] were enriched in the 293T-Dok1 cell population, as measured by the peak intensity. Calculation of SILAC ratios was not possible as no peptides from these proteins were identified in the untransfected cell population.

Of the identified proteins enriched in the 293T-Dok1 cells ~40% are nuclear proteins that are involved in events such as transcription, splicing, DNA replication and nucleic acid metabolism. Although Dok1 is predominantly a cytoplasmic/membrane protein, it has also been shown that a proportion of it is found in the nucleus.[50] The function of Dok1 in the nucleus has not yet been determined, but it may be that these nuclear proteins are linked to its nuclear function. Alternatively, these nuclear proteins may be binding nonspecifically to overexpressed Dok1.

Dok1 is known to function as an adaptor protein in insulin signaling and has recently been shown to have a role in energy metabolism, mediating adipocyte hypertrophy and obesity through modulation of peroxisome proliferator-activated receptor- γ (PPAR-γ) phosphorylation.[55] PPAR-γ is a nuclear receptor that mediates the metabolism of fatty acids and induces genes related to fatty acid metabolism. Antagonising PPAR-γ has been shown to result in a decrease in peroxiredoxin.[56] Interestingly, we identified enriched fatty acid synthase (FAS), peroxiredoxin-1 (PRDX-1) and peroxiredoxin-2 (PRDX-2) as putative Dok1 interactors. It is tempting to speculate that these proteins may link Dok1 to PPAR- γ and their role in energy metabolism.

The Dok1 SILAC experiment in the presence and absence of SU6656, allowed us to identify Dok1 binding partners whose interaction with Dok1 was regulated by SFKs. A total of 341 proteins were identified (<1% FDR) (Supplementary Table S4, Supporting Information). The Dok1 protein itself had a SILAC ratio of 1.05 (heavy/light, where heavy was SU6656-treated). Of the known binding partners of Dok1, PLCγ1 and NCK2 were significantly enriched in the SU6656-treated cells, with SILAC ratios of 2.04 and 2.30, respectively (Table 4). The enrichment of PLCγ1 and NCK2 in the SU6656 treated cells indicates that the inhibition of SFK activity, and thus phosphorylation events mediated by SFKs, has caused an increase in the amount of these proteins bound to Dok1. RasGAP and Csk were not significantly enriched in either cell population (with SILAC ratios of 0.82 and 1.24, respectively), suggesting that these interactions are not SFK-dependent.

For each significant protein hit, their presence in the myc-Dok1 vs untransfected SILAC experiment was checked in order to see whether they may be a contaminant. Where a protein was not significantly enriched in the myc-Dok1 vs untransfected IP (Table 3), the protein was considered a contaminant

Table 4. Proteins Identified in a Myc-Dok1 Immunoprecipitation whose SILAC Ratios are Significantly Changed Due to the Presence of SU6656

protein ID	protein names	unique peptides (seq/mod/labels)	sequence coverage (%)	ratio H/L	ratio H/L significance	ratio $H_{myc\text{-}Dok1}/L_{untransfected}$
	Proteins with reduced SILAC ratios due to presence of SU6656					
IPI00873058	Paired Box 1	2	1.9	0.016	1.05×10^{-21}	[a]
IPI00440577	IGKV2−24 protein	1	3.8	0.042	2.26×10^{-13}	[a]
IPI00798360	SAP domain containing ribonucleoprotein	1	4.3	0.373	1.10×10^{2}	[a]
IPI00104050	Thyroid hormone receptor-associated protein 3	3	2.7	0.391	1.45×10^{2}	[a]
	Proteins with increased SILAC ratios due to presence of SU6656					
IPI00001159	Translational activator GCN1	5	1.4	1.753	4.37×10^{2}	[a]
IPI00003965	Ubiquitin carboxyl-terminal hydrolase 7	7	4.5	1.758	4.29×10^{2}	[b]
IPI00031647	Programmed cell death protein 2-like	2	3.4	1.797	3.69×10^{2}	[b]
IPI00024364	Transportin-1;Importin beta-2	5	3.8	1.823	3.34×10^{2}	[a]
IPI00514856	Ubiquitin-associated protein 2-like	4	1.8	1.834	3.20×10^{2}	[b]
IPI00016932	Phosphatidylinositol-3,4,5-trisphosphate 5-phosphatase 2 (SHIP2)	2	1.4	1.870	2.79×10^{2}	[a]
IPI00221012	Probable ubiquitin carboxyl-terminal hydrolase FAF-X	6	2.7	1.954	2.01×10^{2}	[b]
IPI00020729	Insulin receptor substrate 4 (IRS4)	2	2.1	1.980	1.81×10^{2}	[a]
IPI00383849	Phospholipase C, gamma 1 (PLCγ)	8	4.3	2.036	1.46×10^{2}	[b]
IPI00029705	Gamma-tubulin complex component 2	1	1.2	2.125	1.03×10^{2}	[a]
IPI00306531	NCK adaptor protein 2	1	4.5	2.302	5.11×10^{3}	2.6
IPI00217223	Multifunctional protein ADE2	3	5.8	2.366	3.97×10^{3}	[b]
IPI00410590	LSM14 protein homologue A	2	2.2	2.447	2.89×10^{3}	[a]
IPI00011631	Centromere/kinetochore protein zw10 homologue	2	3.7	3.163	1.79×10^{4}	[a]

[a] Not detected. [b] Detected only in Dok1 immunoprecipitation and not in untransfected control; therefore, no ratio could be calculated.

and removed from the final list (nine proteins). Table 4 shows the remaining 14 proteins that were significantly enriched in the SU6656 treated cells and the 4 proteins that were enriched in the non-SU6656 treated cells. A number of proteins are absent in the myc-Dok1 vs untransfected SILAC experiment (Table 4). In these cases, the possibility remains that the protein may not be a true Dok1 interacting partner, an important consideration when selecting proteins for further biological analysis.

The shuttling of Dok1 between the nucleus and cytoplasm has been shown to be dependent on Src-mediated tyrosine phosphorylation.[50] Phosphorylation of Dok1 by Src causes accumulation of Dok1 in the cytoplasm, assumed to be caused by an inhibition of nuclear import.[50] Interestingly, our data shows that, in the presence of the SFK inhibitor, SU6656, Dok1 bound to more nuclear proteins than in the absence of SU6656. The inhibition of nuclear import due to Src-phosphorylation is presumably due to a lack of interaction with nuclear import transporters. Our data shows an increased amount of Dok1-bound transportin-1, a nuclear import protein, in the absence of Src-induced phosphorylation, consistent with Src-dependent inhibition of nuclear import. However, we note that transportin-1 was not identified as a Dok1-binding protein in the previous experiment; therefore, we cannot be certain that this is a true Dok1 interactor.

IRS4 and SHIP2 were also found enriched in SU6656 treated cells, suggesting that they may bind to Dok1 directly or indirectly in a SFK-dependent manner. Dok1 has not previously been linked to either protein, although all three proteins play a role in insulin signaling[47,48,57,58] and both IRS4 and SHIP2 play a role in FGF/FGFR signaling.[24] Although a direct link between Dok1 and IRS4 has not been previously reported, IRS4 is known to interact with CRKL, which is also a known binding partner of Dok1.[59] The quantitative proteomics approach described here has not only identified additional putative, binding partners of Dok1 but has also provided information about the regulation of these interactions by SFKs. Future studies will be needed to investigate the role of the novel SFK-dependent phosphorylation sites in these interactions.

Conclusions

We have implemented a differential phosphoproteomics approach for dissection of the SFK-mediated interaction network within the FGF signaling pathway. We have focused on those phosphorylation sites which are dependent on activation of SFK activity and then on Dok1, with the identification of both SFK-dependent and independent sites of phosphorylation, and SFK-dependent Dok1 binding partners. The study has revealed the phosphorylation of multiple downstream kinases and adaptor/scaffolding proteins and has identified a significant number of proteins potentially involved in FGF signaling for further functional scrutiny. We note that the final protein-targeted step in our approach can be used to further characterize any of the proteins showing SFK-dependency that we have identified in our global analysis. Indeed, data from such experiments could be combined to provide a detailed tyrosine phosphorylation map of events occurring within the Src-mediated node of FGFR signaling. The experimental approach employed in this study is readily applicable to deeper analysis of both the FGF and other receptor tyrosine kinases.

Supplementary Methods

Peptide and Protein Identification and Quantitation. Antiphosphotyrosine IP (SILAC). Fifteen raw files were analyzed by MaxQuant, 4 were following phosphopeptide enrichment (and therefore searched allowing phosphorylation as a variable modification). Eleven were either flow-throughs from enrichments or unenriched controls (therefore searched without allowing phosphorylation). Three experiments (13 raw files) employed Lys6, Arg10 labels, while one experiment employed only Lys6 label (2 raw files). All 15 files were combined in the 'Identify' step. An experimental design template was used to mark raw files as being from experiment 1, 2, 3, or 4 and also to indicate that the labeling in experiment 3 was inverted. Identifications were filtered using a peptide FDR of 0.01 and a protein FDR of 1.00 (no filtering at the protein level). Supplementary Table S1 (Supporting Information) was created from the evidence.txt output for all four experiments, by sorting according to phospho (Y) site ID. Supplementary Table S2

(Supporting Information) was created from the evidence.txt output for all dual labeled experiments, by sorting according to phospho (Y) site ID and SILAC ratio. Reverse hits and contaminants are not shown. All ratios obtained from MaxQuant were adjusted using a correction factor to allow for mixing error. This correction factor was calculated by combining all unenriched pre-IP control samples and normalizing peptide ratios so that the median of their logarithms is zero. In order to calculate the probability cut-offs ($p = 0.05$), the value for 2 × the standard deviation of the control ratio logarithms was calculated. Ratios were deemed significantly changed if they were <0.616 or >1.624. The correction factor was then applied to the enriched samples, and the means of the corrected ratio logarithms for each peptide were calculated. Variability (%) was calculated using the standard deviation of the natural logarithms of the SILAC ratios, multiplied by 100.

Myc-Dok1 IP Plus/Minus Src Drug (SILAC). Two separate experiments were carried out, resulting in 41 raw files. These were analyzed by MaxQuant, 3 were following phosphopeptide enrichment (and therefore searched allowing phosphorylation as a variable modification). Thiry-six were either gel-slices with no TiO_2 enrichment or flow-throughs from enrichments, and two were pre-IP control samples (therefore searched without allowing phosphorylation). Both experiments employed Lys6, Arg10 labels. All 41 files were combined in the 'Identify' step. To obtain the phosphorylation-specific output columns, the phosphorylated samples were selected to be at the top of the list of files for 'Identify' to process. Identifications were filtered using a peptide FDR of 0.01 and a protein FDR of 0.01. An experimental design template was used to mark raw files as being from experiment 1 or 2. Supplementary Table S3 (Supporting Information) was created from the proteingroups.txt output, by sorting according to normalized SILAC Ratio. Reverse hits and contaminants are not shown. For the enriched Dok1 gel slices, a correction factor was applied to each peptide ratio, calculated from nonenriched pre-IP control samples as described above. Ratios were deemed significantly changed if they were <0.612 or >1.635.

Myc-Dok1 IP versus Untransfected (SILAC). Two separate experiments were carried out, resulting in 34 raw files. These were analyzed by MaxQuant, 2 were following phosphopeptide enrichment (and therefore searched allowing phosphorylation as a variable modification). Thirty-two were either gel-slices with no TiO_2 enrichment or flow-throughs from enrichments (therefore searched without allowing phosphorylation). Both experiments employed Lys6, Arg10 labels. All 34 files were combined in the 'Identify' step. In order to obtain the phosphorylation-specific output columns, the phosphorylated samples were selected to be at the top of the list of files for 'Identify'. Identifications were filtered using a peptide FDR of 0.01 and a protein FDR of 0.01. An experimental design template was used to mark raw files as being from experiment 1 or 2. Supplementary Table S4 (Supporting Information) was created from the proteingroups.txt output, by sorting according to normalized SILAC Ratio. Reverse hits and contaminants are not shown.

Acknowledgment. The authors would like to gratefully acknowledge Andrew Jones and Sue Brewer for technical support, and EU Endotrack (S.M.M.S.), Cancer Research UK (D.L.C., J.K.H.) and the Wellcome Trust (074131) (H.J.C.) for funding.

Supporting Information Available: Supplementary Table S1, identification of phosphotyrosine peptides from SILAC ± SU6656. Supplementary Table S2, quantitation of phosphotyrosine peptides from SILAC ± SU6656. Supplementary Table S3, proteins identified in the myc-Dok1 vs untransfected SILAC experiment. Supplementary Table S4, proteins identified in the myc-Dok1 ± SU6656 SILAC experiment. Supplementary Figure S1, Overlap of phosphotyrosine peptide identification in four SILAC repeat experiments. Supplementary Figure S2, Overlap of phosphotyrosine peptide identification in three SILAC repeat experiments. This material is available free of charge via the Internet at http://pubs.acs.org.

References

(1) Itoh, N.; Ornitz, D. M. Functional evolutionary history of the mouse Fgf gene family. *Dev. Dyn.* **2008**, *237* (1), 18–27.
(2) Beenken, A.; Mohammadi, M. The FGF family: biology, pathophysiology and therapy. *Nat. Rev. Drug Discovery* **2009**, *8* (3), 235–53.
(3) Ornitz, D. M.; Itoh, N. Fibroblast growth factors. *Genome Biol.* **2001**, *2* (3), 3005.1−3005.12.
(4) Grose, R.; Dickson, C. Fibroblast growth factor signaling in tumorigenesis. *Cytokine Growth Factor Rev.* **2005**, *16* (2), 179–86.
(5) Katoh, M. Cancer genomics and genetics of FGFR2 (Review). *Int. J. Oncol.* **2008**, *33* (2), 233–7.
(6) Eswarakumar, V. P.; Lax, I.; Schlessinger, J. Cellular signaling by fibroblast growth factor receptors. *Cytokine Growth Factor Rev.* **2005**, *16* (2), 139–49.
(7) Gotoh, N. Regulation of growth factor signaling by FRS2 family docking/scaffold adaptor proteins. *Cancer Sci.* **2008**, *99* (7), 1319–25.
(8) Kouhara, H.; Hadari, Y. R.; Spivak-Kroizman, T.; Schilling, J.; Bar-Sagi, D.; Lax, I.; Schlessinger, J. A lipid-anchored Grb2-binding protein that links FGF-receptor activation to the Ras/MAPK signaling pathway. *Cell* **1997**, *89* (5), 693–702.
(9) Hadari, Y. R.; Kouhara, H.; Lax, I.; Schlessinger, J. Binding of Shp2 tyrosine phosphatase to FRS2 is essential for fibroblast growth factor-induced PC12 cell differentiation. *Mol. Cell. Biol.* **1998**, *18* (7), 3966–73.
(10) Ong, S. H.; Hadari, Y. R.; Gotoh, N.; Guy, G. R.; Schlessinger, J.; Lax, I. Stimulation of phosphatidylinositol 3-kinase by fibroblast growth factor receptors is mediated by coordinated recruitment of multiple docking proteins. *Proc. Natl. Acad. Sci. U.S.A.* **2001**, *98* (11), 6074–9.
(11) Lamothe, B.; Yamada, M.; Schaeper, U.; Birchmeier, W.; Lax, I.; Schlessinger, J. The docking protein Gab1 is an essential component of an indirect mechanism for fibroblast growth factor stimulation of the phosphatidylinositol 3-kinase/Akt antiapoptotic pathway. *Mol. Cell. Biol.* **2004**, *24* (13), 5657–66.
(12) Mohammadi, M.; Honegger, A. M.; Rotin, D.; Fischer, R.; Bellot, F.; Li, W.; Dionne, C. A.; Jaye, M.; Rubinstein, M.; Schlessinger, J. A tyrosine-phosphorylated carboxy-terminal peptide of the fibroblast growth factor receptor (Flg) is a binding site for the SH2 domain of phospholipase C-gamma 1. *Mol. Cell. Biol.* **1991**, *11* (10), 5068–78.
(13) Vecchione, A.; Cooper, H. J.; Trim, K. J.; Akbarzadeh, S.; Heath, J. K.; Wheldon, L. M. Protein partners in the life history of activated fibroblast growth factor receptors. *Proteomics* **2007**, *7* (24), 4565–78.
(14) Sandilands, E.; Akbarzadeh, S.; Vecchione, A.; McEwan, D. G.; Frame, M. C.; Heath, J. K. Src kinase modulates the activation, transport and signalling dynamics of fibroblast growth factor receptors. *EMBO Rep.* **2007**, *8* (12), 1162–9.
(15) Olsen, J. V.; Blagoev, B.; Gnad, F.; Macek, B.; Kumar, C.; Mortensen, P.; Mann, M. Global, in vivo, and site-specific phosphorylation dynamics in signaling networks. *Cell* **2006**, *127* (3), 635–48.
(16) Bodenmiller, B.; Malmstrom, J.; Gerrits, B.; Campbell, D.; Lam, H.; Schmidt, A.; Rinner, O.; Mueller, L. N.; Shannon, P. T.; Pedrioli, P. G.; Panse, C.; Lee, H. K.; Schlapbach, R.; Aebersold, R. PhosphoPep-a phosphoproteome resource for systems biology research in Drosophila Kc167 cells. *Mol. Systems Biol.* **2007**, *3*, 139.
(17) Zhai, B.; Villen, J.; Beausoleil, S. A.; Mintseris, J.; Gygi, S. P. Phosphoproteome analysis of Drosophila melanogaster embryos. *J. Proteome Res.* **2008**, *7* (4), 1675–82.
(18) Collins, M. O.; Yu, L.; Choudhary, J. S. Analysis of protein phosphorylation on a proteome-scale. *Proteomics* **2007**, *7* (16), 2751–68.

(19) Smith, J. C.; Figeys, D. Recent developments in mass spectrometry-based quantitative phosphoproteomics. *Biochem Cell Biol* **2008**, *86* (2), 137–48.
(20) Blagoev, B.; Kratchmarova, I.; Ong, S. E.; Nielsen, M.; Foster, L. J.; Mann, M. A proteomics strategy to elucidate functional protein-protein interactions applied to EGF signaling. *Nat. Biotechnol.* **2003**, *21* (3), 315–8.
(21) Amanchy, R.; Kalume, D. E.; Iwahori, A.; Zhong, J.; Pandey, A. Phosphoproteome analysis of HeLa cells using stable isotope labeling with amino acids in cell culture (SILAC). *J. Proteome Res.* **2005**, *4* (5), 1661–71.
(22) Cox, J.; Mann, M. MaxQuant enables high peptide identification rates, individualized p.p.b.-range mass accuracies and proteome-wide protein quantification. *Nat. Biotechnol.* **2008**, *26* (12), 1367–72.
(23) Sweet, S. M.; Bailey, C. M.; Cunningham, D. L.; Heath, J. K.; Cooper, H. J. Large scale localization of protein phosphorylation by use of electron capture dissociation mass spectrometry. *Mol. Cell. Proteomics* **2009**, *8* (5), 904–12.
(24) Hinsby, A. M.; Olsen, J. V.; Mann, M. Tyrosine phosphoproteomics of fibroblast growth factor signaling: a role for insulin receptor substrate-4. *J. Biol. Chem.* **2004**, *279* (45), 46438–47.
(25) Hinsby, A. M.; Olsen, J. V.; Bennett, K. L.; Mann, M. Signaling initiated by overexpression of the fibroblast growth factor receptor-1 investigated by mass spectrometry. *Mol. Cell. Proteomics* **2003**, *2* (1), 29–36.
(26) Rush, J.; Moritz, A.; Lee, K. A.; Guo, A.; Goss, V. L.; Spek, E. J.; Zhang, H.; Zha, X. M.; Polakiewicz, R. D.; Comb, M. J. Immunoaffinity profiling of tyrosine phosphorylation in cancer cells. *Nat. Biotechnol.* **2005**, *23* (1), 94–101.
(27) Boeri Erba, E.; Matthiesen, R.; Bunkenborg, J.; Schulze, W. X.; Di Stefano, P.; Cabodi, S.; Tarone, G.; Defilippi, P.; Jensen, O. N. Quantitation of multisite EGF receptor phosphorylation using mass spectrometry and a novel normalization approach. *J. Proteome Res.* **2007**, *6* (7), 2768–85.
(28) Leroy, C.; Fialin, C.; Sirvent, A.; Simon, V.; Urbach, S.; Poncet, J.; Robert, B.; Jouin, P.; Roche, S. Quantitative phosphoproteomics reveals a cluster of tyrosine kinases that mediates SRC invasive activity in advanced colon carcinoma cells. *Cancer Res.* **2009**, *69* (6), 2279–86.
(29) Luo, W.; Slebos, R. J.; Hill, S.; Li, M.; Brabek, J.; Amanchy, R.; Chaerkady, R.; Pandey, A.; Ham, A. J.; Hanks, S. K. Global impact of oncogenic Src on a phosphotyrosine proteome. *J. Proteome Res.* **2008**, *7* (8), 3447–60.
(30) Amanchy, R.; Zhong, J.; Hong, R.; Kim, J. H.; Gucek, M.; Cole, R. N.; Molina, H.; Pandey, A., Identification of c-Src tyrosine kinase substrates in platelet-derived growth factor receptor signaling. *Mol. Oncol.* **2009**, *3* (5−6), 439−50.
(31) Bendall, S. C.; Hughes, C.; Stewart, M. H.; Doble, B.; Bhatia, M.; Lajoie, G. A. Prevention of amino acid conversion in SILAC experiments with embryonic stem cells. *Mol. Cell. Proteomics* **2008**, *7* (9), 1587–97.
(32) Cox, J.; Matic, I.; Hilger, M.; Nagaraj, N.; Selbach, M.; Olsen, J. V.; Mann, M. A practical guide to the MaxQuant computational platform for SILAC-based quantitative proteomics. *Nat. Protoc.* **2009**, *8* (5), 904–12.
(33) Bailey, C. M.; Sweet, S. M.; Cunningham, D. L.; Zeller, M.; Heath, J. K.; Cooper, H. J. SLoMo: Automated Site Localization of Modifications from ETD/ECD Mass Spectra. *J. Proteome Res.* **2009**, *8*, 1965–71.
(34) Bromann, P. A.; Korkaya, H.; Courtneidge, S. A. The interplay between Src family kinases and receptor tyrosine kinases. *Oncogene* **2004**, *23* (48), 7957–68.
(35) Li, X.; Brunton, V. G.; Burgar, H. R.; Wheldon, L. M.; Heath, J. K. FRS2-dependent SRC activation is required for fibroblast growth factor receptor-induced phosphorylation of Sprouty and suppression of ERK activity. *J. Cell Sci.* **2004**, *117* (Pt 25), 6007–17.
(36) Sandilands, E.; Frame, M. C. Endosomal trafficking of Src tyrosine kinase. *Trends Cell Biol.* **2008**, *18* (7), 322–9.
(37) Blake, R. A.; Broome, M. A.; Liu, X.; Wu, J.; Gishizky, M.; Sun, L.; Courtneidge, S. A. SU6656, a selective src family kinase inhibitor, used to probe growth factor signaling. *Mol. Cell. Biol.* **2000**, *20* (23), 9018–27.
(38) Hornbeck, P. V.; Chabra, I.; Kornhauser, J. M.; Skrzypek, E.; Zhang, B. PhosphoSite: A bioinformatics resource dedicated to physiological protein phosphorylation. *Proteomics* **2004**, *4* (6), 1551–61.
(39) Maa, M. C.; Lai, J. R.; Lin, R. W.; Leu, T. H. Enhancement of tyrosyl phosphorylation and protein expression of eps8 by v-Src. *Biochim. Biophys. Acta* **1999**, *1450* (3), 341–51.
(40) Thomas, S. M.; Brugge, J. S. Cellular functions regulated by Src family kinases. *Annu. Rev. Cell Dev. Biol.* **1997**, *13*, 513–609.
(41) Lombardo, C. R.; Consler, T. G.; Kassel, D. B. In vitro phosphorylation of the epidermal growth factor receptor autophosphorylation domain by c-src: identification of phosphorylation sites and c-src SH2 domain binding sites. *Biochemistry* **1995**, *34* (50), 16456–66.
(42) Keshava Prasad, T. S.; Goel, R.; Kandasamy, K.; Keerthikumar, S.; Kumar, S.; Mathivanan, S.; Telikicherla, D.; Raju, R.; Shafreen, B.; Venugopal, A.; Balakrishnan, L.; Marimuthu, A.; Banerjee, S.; Somanathan, D. S.; Sebastian, A.; Rani, S.; Ray, S.; Harrys Kishore, C. J.; Kanth, S.; Ahmed, M.; Kashyap, M. K.; Mohmood, R.; Ramachandra, Y. L.; Krishna, V.; Rahiman, B. A.; Mohan, S.; Ranganathan, P.; Ramabadran, S.; Chaerkady, R.; Pandey, A. Human Protein Reference Database--2009 update. *Nucleic Acids Res.* **2009**, *69* (6), 2279–86.
(43) Taylor, S. J.; Shalloway, D. An RNA-binding protein associated with Src through its SH2 and SH3 domains in mitosis. *Nature* **1994**, *368* (6474), 867–71.
(44) Richard, S.; Yu, D.; Blumer, K. J.; Hausladen, D.; Olszowy, M. W.; Connelly, P. A.; Shaw, A. S. Association of p62, a multifunctional SH2- and SH3-domain-binding protein, with src family tyrosine kinases, Grb2, and phospholipase C gamma-1. *Mol. Cell. Biol.* **1995**, *15* (1), 186–97.
(45) Chang, J. H.; Wilson, L. K.; Moyers, J. S.; Zhang, K.; Parsons, S. J. Increased levels of p21ras-GTP and enhanced DNA synthesis accompany elevated tyrosyl phosphorylation of GAP-associated proteins, p190 and p62, in c-src overexpressors. *Oncogene* **1993**, *8* (4), 959–67.
(46) Shah, K.; Shokat, K. M. A chemical genetic screen for direct v-Src substrates reveals ordered assembly of a retrograde signaling pathway. *Chem. Biol.* **2002**, *9* (1), 35–47.
(47) Sung, C. K.; Sanchez-Margalet, V.; Goldfine, I. D. Role of p85 subunit of phosphatidylinositol-3-kinase as an adaptor molecule linking the insulin receptor, p62, and GTPase-activating protein. *J. Biol. Chem.* **1994**, *269* (17), 12503–7.
(48) Wick, M. J.; Dong, L. Q.; Hu, D.; Langlais, P.; Liu, F. Insulin receptor-mediated p62dok tyrosine phosphorylation at residues 362 and 398 plays distinct roles for binding GTPase-activating protein and Nck and is essential for inhibiting insulin-stimulated activation of Ras and Akt. *J. Biol. Chem.* **2001**, *276* (46), 42843–50.
(49) Sweet, S. M. M.; Mardakheh, F. K.; Ryan, K. J. P.; Langton, A. J.; Heath, J. K.; Cooper, H. J. Targeted Online Liquid Chromatography Electron Capture Dissociation Mass Spectrometry for the Localization of Sites of in Vivo Phosphorylation in Human Sprouty2. *Anal. Chem.* **2008**, *80* (17), 6650–6657.
(50) Niu, Y.; Roy, F.; Saltel, F.; Andrieu-Soler, C.; Dong, W.; Chantegrel, A. L.; Accardi, R.; Thepot, A.; Foiselle, N.; Tommasino, M.; Jurdic, P.; Sylla, B. S. A nuclear export signal and phosphorylation regulate Dok1 subcellular localization and functions. *Mol. Cell. Biol.* **2006**, *26* (11), 4288–301.
(51) Kashige, N.; Carpino, N.; Kobayashi, R. Tyrosine phosphorylation of p62dok by p210bcr-abl inhibits RasGAP activity. *Proc Natl. Acad. Sci. U.S.A.* **2000**, *97* (5), 2093–8.
(52) Shinohara, H.; Yasuda, T.; Yamanashi, Y. Dok-1 tyrosine residues at 336 and 340 are essential for the negative regulation of Ras-Erk signalling, but dispensable for rasGAP-binding. *Genes Cells* **2004**, *9* (6), 601–7.
(53) Neet, K.; Hunter, T. The nonreceptor protein-tyrosine kinase CSK complexes directly with the GTPase-activating protein-associated p62 protein in cells expressing v-Src or activated c-Src. *Mol. Cell. Biol.* **1995**, *15* (9), 4908–20.
(54) Chen, M.; She, H.; Davis, E. M.; Spicer, C. M.; Kim, L.; Ren, R.; Le Beau, M. M.; Li, W. Identification of Nck family genes, chromosomal localization, expression, and signaling specificity. *J. Biol. Chem.* **1998**, *273* (39), 25171–8.
(55) Hosooka, T.; Noguchi, T.; Kotani, K.; Nakamura, T.; Sakaue, H.; Inoue, H.; Ogawa, W.; Tobimatsu, K.; Takazawa, K.; Sakai, M.; Matsuki, Y.; Hiramatsu, R.; Yasuda, T.; Lazar, M. A.; Yamanashi, Y.; Kasuga, M. Dok1 mediates high-fat diet-induced adipocyte hypertrophy and obesity through modulation of PPAR-gamma phosphorylation. *Nat. Med.* **2008**, *14* (2), 188–93.
(56) Tyagi, S. C.; Rodriguez, W.; Patel, A. M.; Roberts, A. M.; Falcone, J. C.; Passmore, J. C.; Fleming, J. T.; Joshua, I. G. Hyperhomocysteinemic diabetic cardiomyopathy: oxidative stress, remodeling, and endothelial-myocyte uncoupling. *J. Cardiovasc. Pharmacol. Ther.* **2005**, *10* (1), 1–10.
(57) Lavan, B. E.; Fantin, V. R.; Chang, E. T.; Lane, W. S.; Keller, S. R.; Lienhard, G. E. A novel 160-kDa phosphotyrosine protein in

insulin-treated embryonic kidney cells is a new member of the insulin receptor substrate family. *J. Biol. Chem.* **1997**, *272* (34), 21403–7.
(58) Clement, S.; Krause, U.; Desmedt, F.; Tanti, J. F.; Behrends, J.; Pesesse, X.; Sasaki, T.; Penninger, J.; Doherty, M.; Malaisse, W.; Dumont, J. E.; Le Marchand-Brustel, Y.; Erneux, C.; Hue, L.; Schurmans, S. The lipid phosphatase SHIP2 controls insulin sensitivity. *Nature* **2001**, *409* (6816), 92–7.
(59) Koval, A. P.; Karas, M.; Zick, Y.; LeRoith, D. Interplay of the proto-oncogene proteins CrkL and CrkII in insulin-like growth factor-I receptor-mediated signal transduction. *J. Biol. Chem.* **1998**, *273* (24), 14780–7.

PR9010475